Influence of Particulates on Infrared Emission from Tactical Rocket Exhausts

H.F. Nelson*
Air Force Rocket Propulsion Laboratory, Edwards AFB, California

The influence of radiation scattering on the infrared radiation signature of representative plumes from four types of tactical rocket motors is investigated using the recently developed JANNAF Standardized Infrared Radiation Model (SIRRM) numerical code. The plumes are modeled as isothermal cylinders with gas and particle compositions representative of 1) advanced liquid rocket exhausts (HCl, HF/carbon); 2) low-temperature metal fuel solid rocket exhausts (H_2O, HCl, CO/aluminum oxide); 3) reduced smoke low visibility solid rocket exhausts (H_2O, HCl, CO, CO_2/aluminum oxide); and 4) advanced minimum smoke solid rocket exhausts (CO, CO_2, H_2O/zirconium oxide). The signatures of the plumes containing carbon particles are sensitive to the amount of carbon present, but insensitive to the carbon particle size. The signatures of the plumes containing aluminum oxide particles are sensitive to both the particle size and the amount of aluminum oxide present. The emission from the advanced minimum smoke plume becomes increasingly sensitive to particle size and concentration as the particle loading increases.

Nomenclature

b = backscatter fraction
$g(\tau_a, \alpha)$ = gas band model curve of growth for absorption
$I(s)$ = spectral radiance at point s, $W/(cm^2 - Sr - 1/cm)$
I_B = blackbody intensity, $W/(cm^2 - Sr - 1/cm)$
m = particle mass loading, g/cm^3
N = particle number density, $1/cm^3$
P = plume pressure, atm
R = particle radius, μm
s = path length, cm
t = transmission
T = plume temperature, K
W = parameter, see Eq. (3)
W_m = value of W integrated over entire path
X = particle mole fraction
α = fine structure parameter
β, δ = parameters, see Eqs. (9) and (2), respectively
δ_0, δ_m = value of δ at near and far boundaries, respectively
$\Delta\omega$ = spectral interval, $1/cm$
η = band model optical thickness
ρ = particle density, g/cm^3
σ_a, σ_s = absorption and scattering cross sections, respectively, cm^2
τ_a = absorption optical depth
τ_{sb} = backscatter optical depth
ω = wavenumber, $1/cm$

Superscripts

$(\bar{\ })$ = spectral average, see Eq. (7)
$(\ )'$ = dummy integration variable

Introduction

RADIATION emitted from rocket exhaust plumes plays a significant role in missile design because of base heating[1,2] as well as in identification and detection of rockets. Exhausts of solid propellant rockets usually contain substantial amounts of particulate matter that scatters photons, and, therefore, influences the radiation transport processes in the plumes and the emission of radiation from the plumes.[3,4] Radiation scattering also influences the plume flowfield and shock-wave structure,[5] and the aspect angle dependence of the emitted radiation, especially at close to nose-on angles.[6] The retrieval of radial gas temperature and concentration profiles from the plume radiation signature is sensitive to the effects of scattering.[7] The radiation signatures of large power plant plumes are also of interest from an atmospheric environment point of view.[8]

This study investigates the influence of radiation scattering on the infrared plume signatures of several representative rocket motors: 1) advanced liquid rocket plume (ALP) (HCl, HF—carbon); 2) low-temperature metal fuel solid rocket plume (LTMFP) (H_2O, HCl, CO—aluminum oxide); 3) reduced smoke low visibility solid rocket plume (RSP) (H_2O, HCl, CO, CO_2—aluminum oxide); and 4) advanced minimum smoke solid rocket plume (AMSP) (CO, CO_2, H_2O—zirconium oxide). The rocket plumes are classified according to their signature in the visible part of the spectrum as reduced smoke, minimum smoke, etc. The rocket motor pro-

Table 1 Propellant properties—plume composition

	ALP	LTMFP	RSP	AMSP
Propellant	(MHF-3/ClF_5)	(Al/AP)	(HTPB/AP)	(HMX)
Temperature, K	1000	1000	1000	1800
Pressure, atm	1.0	1.0	1.0	1.0
Plume composition	Mole fraction			
Gases				
HCl	0.10	0.13	0.18	—
HF	0.50	—	—	—
H_2	0.20	(0.40)	(0.10)	(0.40)
H_2O	—	0.30	0.40	0.20
CO	—	0.02	0.12	0.10
CO_2	—	—	0.12	0.10
N_2	(0.10)	(0.05)	(0.03)	(0.15)
Particles				
Al_2O_3	—	(0.50)	(0.05)	—
C	(0.10)	—	—	—
ZrO_2	—	—	—	(0.05)

Presented as Paper 82-0913 at the AIAA/ASME 3rd Joint Thermophysics, Fluids, Plasma and Heat Transfer Conference, St. Louis, Mo., June 7-11, 1982; submitted Jan. 31, 1983; revision received Aug. 6, 1983.

*Research Professor. Currently Professor of Aerospace Engineering, Department of Mechanical and Aerospace Engineering, University of Missouri-Rolla, Rolla, Mo. Associate Fellow AIAA.

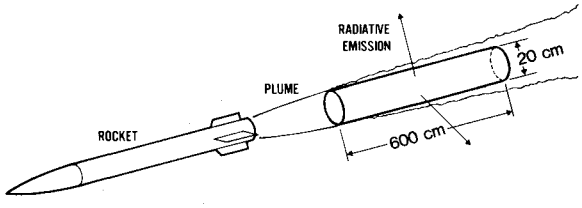

- PLUME MODEL
- ISOTHERMAL
- HOMOGENEOUS
- UNIFORM SIZE PARTICLES

Fig. 1 Schematic of the exhaust plume model.

Table 2 Characteristics of rocket motor exhaust plumes

Particle mole fraction	Particle mass loading, g/cm^3	Particle radius, μm Particle number density, 1/cm^3		
		ALP		
C		0.01	0.05	0.10
0.005	7.39×10^{-7}	7.84 + 10[a]	6.27 + 08	7.84 + 07
0.01	1.49×10^{-6}	1.58 + 11	1.26 + 09	1.58 + 08
0.10	1.63×10^{-5}	1.73 + 12	1.39 + 10	1.73 + 09
		LTMFP		
Al_2O_3		0.10	1.00	5.00
0.001	1.25×10^{-6}	8.08 + 07	8.08 + 04	6.46 + 02
0.01	1.26×10^{-5}	8.15 + 08	8.15 + 05	6.52 + 03
0.10	1.39×10^{-4}	8.96 + 09	8.96 + 06	7.17 + 04
0.50	1.25×10^{-3}	8.07 + 10	8.07 + 07	6.45 + 05
		RSP		
Al_2O_3		0.10	1.00	2.00
0.0005	6.26×10^{-7}	4.04 + 07	4.04 + 04	5.05 + 03
0.005	6.28×10^{-6}	4.05 + 08	4.05 + 05	5.07 + 04
0.05	6.58×10^{-5}	4.25 + 09	4.25 + 06	5.31 + 05
		AMS		
ZrO_2		0.10	1.00	
0.001	8.38×10^{-7}	3.64 + 07	3.64 + 04	
0.01	8.46×10^{-6}	3.67 + 08	3.67 + 05	
0.05	4.41×10^{-5}	1.91 + 09	1.91 + 06	

[a] + 10 means 10^{+10}.

pellant properties and plume compositions are tabulated in Table 1.

The six-flux version of the JANNAF Standardized Infrared Radiation Model (SIRRM) radiation transfer code was used to calculate the infrared radiation emitted from the exhaust plumes.[9-11] SIRRM is a recently developed state-of-the-art numerical code that allows for particle scattering and absorption. The previous plume codes considered the particles to be a pseudogas.

The plume flowfield is shown schematically in Fig. 1. It was modeled as a cylinder with a 20 cm diameter and a 600 cm length. The cylinder was assumed to be isothermal and its gaseous and particle concentrations were taken to be uniform throughout its volume. The particles were assumed to be spherical and all to have the same radius. The radiation signatures were calculated for a matrix of particle sizes and particle number densities for each rocket motor as shown in Table 2.

Analysis

The six-flux SIRRM numerical code is an approximate solution to the radiative transfer equation especially developed to predict the infrared radiation signature of rocket exhaust plumes.[11,12] It allows for 1) the important molecular vibration-rotation bands, 2) Mie scattering, 3) nonhomogeneous particulate and gaseous concentrations, and 4) variable temperatures throughout the plume volume. The SIRRM numerical code approximates the scattering term in the radiative transfer equation using a six-flux model for the scattering phase function. The code employs band modeling for the coupled absorbing and scattering processes of the particulates and molecules. It uses Mie scattering analysis to compute the cross sections for the particulates. The radiative emission from the plume is obtained by transforming the six-flux equations into two-flux form and using a finite difference numerical scheme. Six-flux radiation models have been reviewed by Meador and Weaver.[13] They point out that six-flux calculations sometimes yield poor results due to unrealistic photon trapping, because of the transverse components in the scattering cross sections.

The SIRRM solution is developed in terms of the spectral radiance $I_\omega(s)$ at point s. An approximate solution to the radiation transport equation is obtained as

$$I(0)=2\delta_0\left[(\delta_m+1)\int_0^{W_m}\frac{I_B}{\delta}\exp(W_m-W')\,dW'-(\delta_m-1)\right.$$
$$\left.\times\int_0^{W_m}\frac{I_B}{\delta}\exp(W'-W_m)\,dW'\right]\Big/\left[(\delta_m+1)(\delta_0+1)\exp(W_m)\right.$$
$$\left.-(\delta_m-1)(\delta_0-1)\exp(-W_m)\right] \quad (1)$$

at point $s=0$, where the wavenumber subscript is not shown and where

$$\delta=(1+2b\sigma_s/\sigma_a)^{\frac{1}{2}} \quad (2)$$

and

$$W=\int\delta N\sigma_a\,ds \quad (3)$$

The parameter W_m is the value of W integrated over the entire path from the far boundary to the near boundary ($s=0$).

The SIRRM six-flux solution is derived in terms of the spectral averaged transmission

$$\bar{t}=\exp[-\eta] \quad (4)$$

where η is the band model optical thickness, represented by the empirical expression

$$\eta=g(\bar{\tau}_a,\alpha)\left[1+\frac{2\tau_{sb}}{g(\bar{\tau}_a,\alpha)}\right]^{\frac{1}{2}}$$
$$\times\left[\frac{(\bar{\tau}_a+1)\alpha}{(\bar{\tau}_a+1)\alpha+\frac{1}{8}\tau_{sb}^2\left[1+\frac{g(\bar{\tau}_a,\alpha)}{\bar{\tau}_a}\right]}\right]^{\frac{1}{12}} \quad (5)$$

in the spectral interval $\Delta\omega$. The function η represents the coupled absorption-scattering band modeling. In the six-flux SIRRM numerical solution η from Eq. (5) replaces W in Eq. (1).

A detailed study of empirical forms for η was made because the exact formulation yielded an integral that had to be evaluated numerically. The empirical expression for η was required to agree with the numerical evaluation and to have

the correct asymptotic behavior for 1) weak scattering limit ($\tau_{sb} \ll \bar{\tau}_a$), 2) constant absorption coefficient approximation for any band model [$\alpha \to \infty, g(\bar{\tau}_a, \alpha) \to \bar{\tau}_a$], and 3) strong-line, large scattering limit ($\bar{\tau}_a/\alpha \to \infty, \tau_{sb} \to \infty$).[11,12] The exponential-tailed $1/S$ random band model was used to model the molecular bands. Details on the accuracy of the empirical expression for η and the way that $\bar{t}$ fits into the SIRRM formulation are available in Refs. 11 and 12.

It is shown in the limiting case of δ constant along the path that the average emission in a spectral interval, $\Delta\omega$ can be written

$$\bar{\epsilon} \simeq \frac{1 - \exp(-\eta)}{1 + 0.5(\bar{\delta} - 1)(1 + \exp(-\eta))} \tag{6}$$

where $\bar{\delta}$ is the spectral average of δ

$$\bar{\delta} = \frac{1}{\Delta\omega} \int_{\Delta\omega} \delta \, d\omega \tag{7}$$

The SIRRM code was developed with the goal of being capable of predicting the infrared radiation from tactical and strategic missile exhaust plumes within a factor-of-two accuracy over the 2-25 μm spectral range. It has been tested against well-characterized experimental data which simulates the radiative scattering, emission, and absorption for hot gas-particle systems over a range of conditions representative of solid propellant rocket exhaust plumes.[11,12,14] The code also has been checked against the output of previous codes.[12] The code has been validated and it more than meets its design goal of a factor-of-two accuracy over the 2-25 μm spectral range. The data base for molecular and particle properties is also being improved periodically. This serves to increase the predictive accuracy of the code.

The particulate concentration in rocket exhaust flowfields is defined in terms of the particle mass loading

$$m = 4\pi R^3 \rho N/3 \tag{8}$$

The values of ρ are 3.70, 2.25, and 5.50 g/cm^3 for Al_2O_3, C, and ZrO_2, respectively. The relationship between the particle mole fraction and particle mass loading is dependent on the gaseous properties of the flowfield. For the assumptions made in this study the particle mole fraction can be written as[15]

$$X = 1/[1 + \beta P/(mT)] \tag{9}$$

The value of β is 1.250 for Al_2O_3, 0.1471 for C, and 1.508 for ZrO_2. Equation (9) relates the particle mole fraction to the particle mass loading and the plume thermodynamic conditions for the assumptions made in this study.

Results and Discussion

This section contains a general discussion of the infrared radiation emission from the four model plumes discussed in the Introduction. All of the spectral data presented is for a path through the diameter of the plume (spectral radiance) and the observation point is at infinity. The effects of transmission through the intervening atmosphere are not included in the calculations. The aspect angle is 90 deg. The particle sizes are defined in terms of the particle radius in micrometers.

The propellant and plume composition for each of the model plumes is given in Table 1. The mole fractions in parentheses are adjustable so that the sum of the mole fractions is unity.

Advanced Liquid (Carbon/HF, HCl) Plume

The ALP represents a typical plume from an advanced liquid tactical rocket motor using MHF-3 fuel with ClF_5 as the oxidizer. The MHF-3 fuel composition is approximately 85% CH_6N_2 (monometholhydrazine—MMH) and 15% N_2H_4 (hydrazine). This propellant yields plumes with high concentrations of HF and HCl, both of which have active infrared molecular bands, as well as hydrogen and nitrogen, which do not radiate in the infrared. (See Table 1.) The carbon in the fuel is the source of the carbon in the exhaust. The carbon mole fraction in the plume can become as high as 0.10.

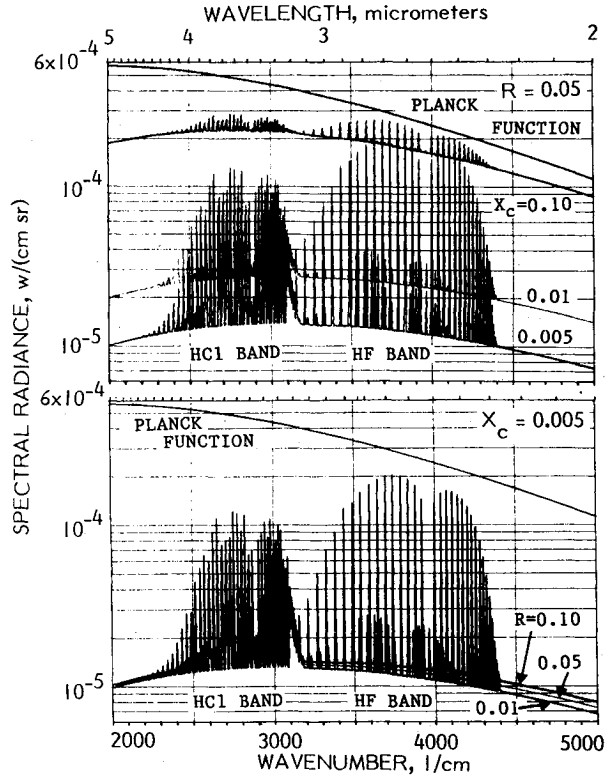

Fig. 2 Spectral radiance from ALP. Upper figure for 0.05-μm carbon particles at mole fractions of 0.005, 0.01, and 0.10. Lower figure for a carbon mole fraction of 0.005 for 0.01-, 0.05-, and 0.10-μm carbon particles.

The spectral radiance from the ALP is shown in Fig. 2 as a function of wavenumber. The corresponding wavelength is shown at the top of the figure for reference. The top part of the figure shows the emitted radiation intensity for plumes containing 0.05 μm carbon particles for three carbon particle mole fractions (0.005, 0.01, and 0.10). The equivalent mass loading levels are 7.39×10^{-7}, 1.49×10^{-6}, and 1.63×10^{-5} g/cm^3, respectively. The bottom part of the figure shows the radiance emitted from plumes with a carbon particle mole fraction of 0.005 for three particle sizes. The Planck function for the plume thermodynamic conditions is also shown on the figure for reference.

Figure 2 shows the emission from the molecular bands of HF at 2.5 μm and of HCl at 3.5 μm. The radiation emission is very sensitive to the carbon particle mole fraction. It increases almost linearly with the particle concentration because carbon has a high absorption coefficient; consequently, carbon is a good emitter. The plume emission is sensitive to particle loading and approaches that of a blackbody at large loadings. The spectral radiance is not very sensitive to changes in carbon particle radius at a constant particle loading.

Figure 3 shows the band model curve of growth for plumes with 0.05 μm carbon particles at the three concentrations of interest. The average value of η for a given wavenumber involves band modeling for combined absorption and scattering in wavenumber intervals of 5 1/cm, and is calculated for a path along the plume diameter. Since the plumes considered herein are homogeneous and isothermal, values of η, along any path through the plume, are directly proportional to the values of η along the diameter. The average transmission and

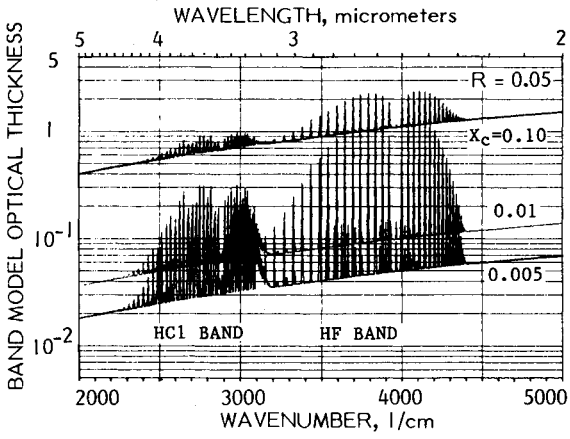

Fig. 3 Spectral variation of the band model optical thickness across the plume diameter for ALP with 0.05-μm carbon particles at mole fractions of 0.005, 0.01, and 0.10.

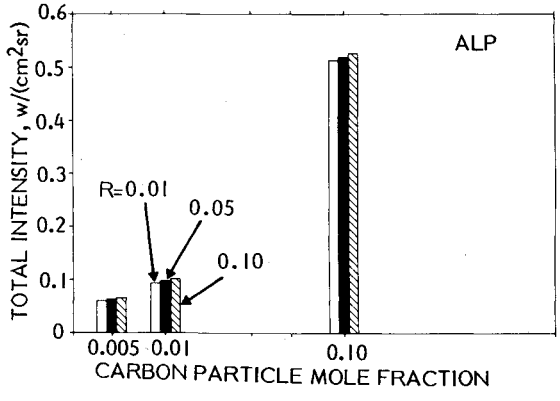

Fig. 4 Integrated radiative emission in the 2000-5000 1/cm wavenumber band from ALP as a function of particle size and concentration.

emission at a given wavenumber are directly related to η as given by Eqs. (4) and (6). The change in η when the carbon particle concentration is changed is entirely due to the particles. The molecular gas absorption remains constant because the gas composition does not change.

The total radiation intensity emitted in the 2000-5000 1/cm wavenumber band is shown as a function of particle size and concentration in Fig. 4. It is defined as the integral of the spectral radiance as shown in Fig. 2 over the wavenumber interval. The height of each bar is equal to the area under the corresponding curve of Fig. 2. Each set of bars represents the effect of changing particle size while keeping the particle mole fraction constant. The total intensity increases slightly as the particle size increases at constant particle loading. This is due in part to the slightly larger absorption coefficient of the larger particles. However, the scattering coefficient also increases with particle size resulting in a larger extinction coefficient. Both of these combine to increase η slightly. This results in an increase in the emission because η is small. The plume is optically thin except in the HF band; therefore, emission increases with increasing η. The intensity also increases for constant-sized particles as the particle loading increases. This is due to the increase in particle absorption because the particle absorption is related directly to the particle concentration.

Low-Temperature Metal Fuel (Al_2O_3/H_2O, HCl, CO) Plume

The LTMFP represents a typical section of plume from a reduced smoke, metal fuel, solid propellant, tactical rocket motor. The section of plume is located near the nozzle exit prior to afterburning. The basic propellant that produces this type of plume is a mixture of aluminum with AP (ammonium

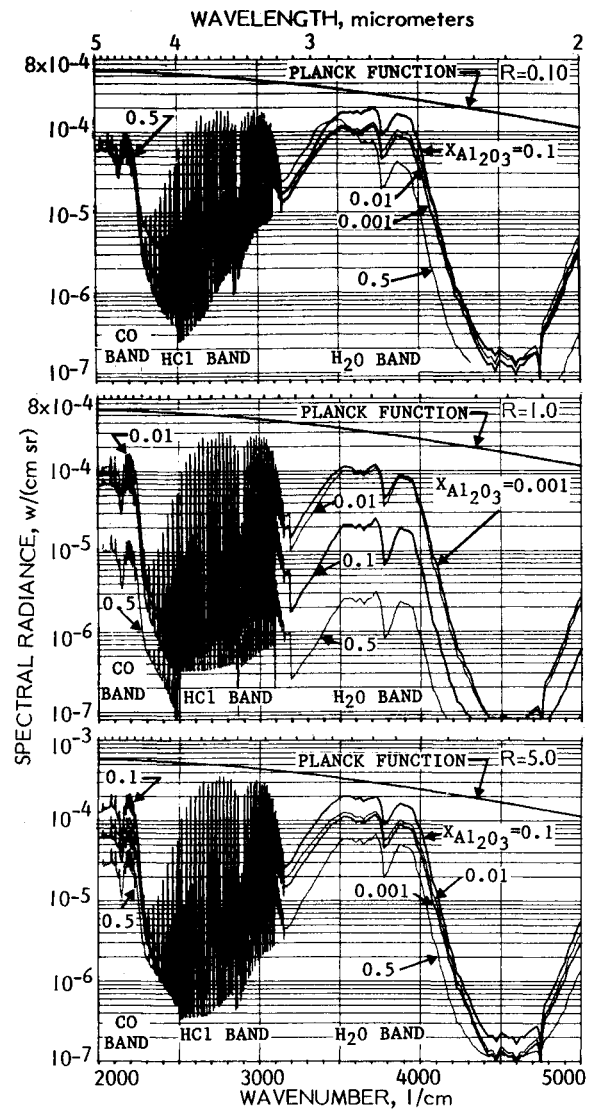

Fig. 5 Spectral radiance from LTMFP at mole fractions of 0.001, 0.01, 0.10, and 0.50 for 0.10-, 1.0-, and 5.0-μm aluminum oxide particles.

perchlorate NH_3ClOHO_3). The aluminum burns to form the Al_2O_3 that exists in the plume. Typical mole fractions of Al_2O_3 in the exhaust can reach 0.10 or more. The infrared radiation from this plume is emitted by the H_2O, HCl, and CO gases in the plume. The most important non-infrared radiating gases are H_2 and N_2, as shown in Table 1.

The spectral radiance from the LTMFP is shown in Fig. 5 as a function of wavenumber for 0.1, 1.0, and 5.0 μm Al_2O_3 particles. Each part of the figure contains results for four mole fractions of aluminum oxide particles. The spectral bands of the gases in the plume are labeled on the figures (the 4.6-μm CO band, the 3.5-μm HCl band, and the 2.7-μm H_2O band). Only the mole fraction of the Al_2O_3 particles is changed. The Al_2O_3 particles are essentially pure scatters; consequently, changing the particle loading does not change the local emission; it only changes the scattering.

The trends shown in Fig. 5 can be explained by considering the band modeling extinction in the plume. Figure 6 shows η along the plume diameter for the plumes shown in Fig. 5. Inspection of Fig. 6 for the 0.1-μm particles leads one to expect that the spectral emission from the plumes with particle mole fractions of 0.001 and 0.01 to be about the same, and that from the plume with a particle mole fraction of 0.1 to be slightly larger, because the plumes remain optically thin in the molecular bands where the emission occurs. The increase in particle loading increases η, but not enough to reduce the

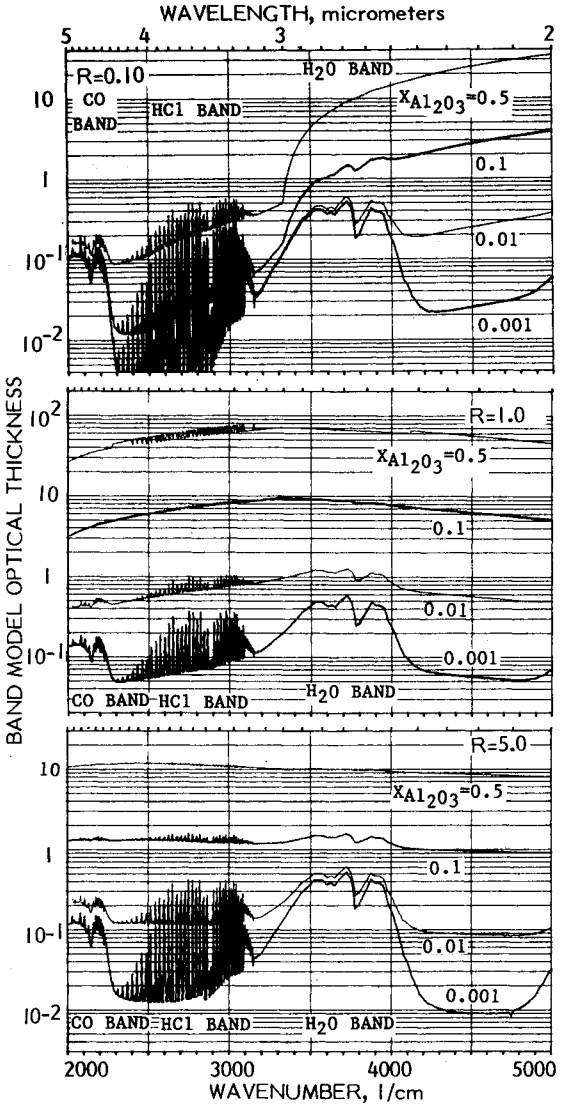

Fig. 6 Spectral variation of the band model optical thickness across the plume diameter for LTMFP at mole fractions of 0.001, 0.01, 0.10, and 0.50 for 0.10-, 1.0-, and 5.0-μm aluminum oxide particles.

radiation emitted from the plume. When the particle mole fraction is increased to 0.5 scattering dominates absorption-emission. The attenuation becomes large and only a small amount of radiation escapes from the plume. The radiation emitted near the plume core is strongly scattered and very little of it escapes from the plume as emitted energy. This is especially true in the water band where η is greater than 10. Figure 5 shows that radiance from the plumes with Al_2O_3 mole fractions of 0.5 becomes less than the radiance from the more lightly loaded plumes at wavenumbers greater than 3500.

Figure 6 also shows the value of η for plumes with 1- and 5-μm particles as a function of wavenumber for the four particle mole fractions of interest. The values of η are, on average, considerably larger than they were for the 0.1-μm particles at the same mole fraction and wavenumber; however, the maximum emission occurs from the plume whose value of η is roughly unity. At larger particle mole fractions the plume emission decreases because only radiation emitted near the outer edge of the plume can escape from the plume. Figure 5 shows that the plumes with 1- and 5-μm particles at a 0.5 particle mole fraction have a considerably reduced emission because of the intense scattering.

Figure 7 shows the total radiation emitted in the 2000-5000 1/cm wavenumber band as a function of particle concentration and size. The radiation emission from plumes containing

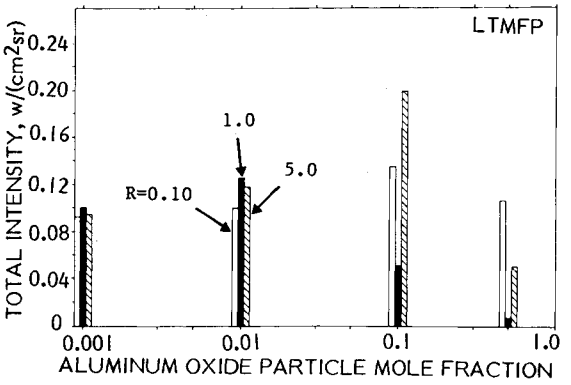

Fig. 7 Integrated radiative emission in the 2000-5000 1/cm wavenumber band from LTMFP as a function of particle size and concentration.

0.1- and 5-μm particles increases with particle mole fraction up to mole fractions of 0.1, because these plumes tend to be optically thin. For larger particle mole fractions scattering becomes so intense that only radiation emitted near the outer edges of the plume escapes, thus reducing the emission. The same phenomenon occurs for the 1-μm particles; however, it occurs at lower particle concentration.

The effect of changing particle size while keeping the particle loading constant is also shown in Fig. 7. The 1-μm particles have a larger scattering cross section than the 0.1- and 5.0-μm particles; therefore, when the plume is optically thin and lightly loaded the plumes with 1-μm particles emit more radiation than the other plumes. As the particle concentration increases the plumes with 1-μm particles become optically thick first. Hence, their emission becomes less than that from the plumes with 0.1- and 5.0-μm particles at lower particle concentrations.

Reduced Smoke Solid Rocket Motor (Al_2O_3/H_2O, CO_2, CO, HCl) Plume

The RSP represents a typical plume from a representative reduced smoke propellant near the nozzle exit. The basic propellant consists of approximately 10% HTPB (hydroxyl terminated polybutadiene) and 85% AP (ammonium perchlorate). In this case Al_2O_3 is added to the propellant for combustion stability which accounts for the aluminum oxide in the plume. The major infrared emission in the exhaust is from H_2O, HCl, CO_2, and CO molecules. The radiative inactive exhaust gases are N_2 and H_2, as seen in Table 1.

Figure 8 shows the spectral radiance from the RSP as a function of Al_2O_3 mole fraction for 0.1-, 1.0-, and 2.0-μm particles. Results are shown for three Al_2O_3 mole fractions: 0.0005, 0.005, and 0.05. The emission is from active molecular bands of the plume gases: The CO band at 4.6 μm, the CO_2 band at 4.3 μm, the HCl band at 3.6 μm, and the H_2O and CO_2 bands at 2.7 μm. Note the emission is black in the spectral region of the 4.3 CO_2 band.

The Al_2O_3 mole fractions are quite small in these plumes; consequently, the plume emission increases slightly as the Al_2O_3 concentration increases. This occurs over essentially the entire wavenumber range for all three particle sizes. Figure 9 shows the spectral variation of η for these cases. η increases with particle loading, reaching a maximum of about unity for an Al_2O_3 mole fraction of 0.05. This implies that further increases in particle loading would tend to reduce the radiative emission across the entire spectrum except in the CO_2 band, where the emission is black.

The RSP radiates like a blackbody in the spectral region near 4.3 μm because the plume absorption coefficient is very large due to the CO_2 concentration. This implies that the plume albedo is low. Scattering does not influence the emission until it becomes strong enough to increase the plume albedo to close to unity. Then the scattering begins to dominate

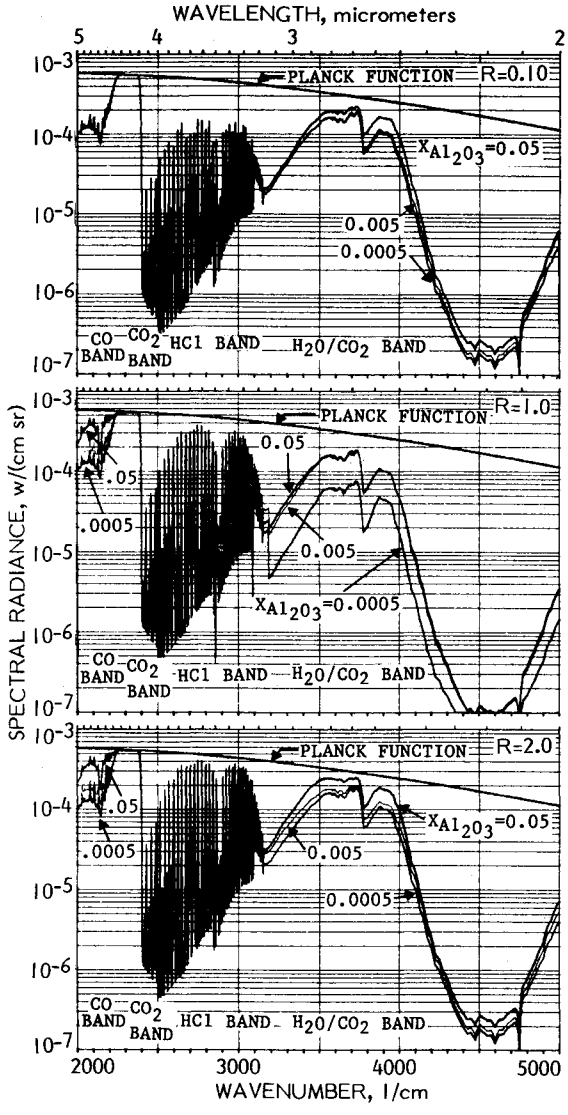

Fig. 8 Spectral radiance from RSP at mole fractions of 0.0005, 0.005, and 0.05 for 0.10-, 1.0-, and 2.0-μm aluminum oxide particles.

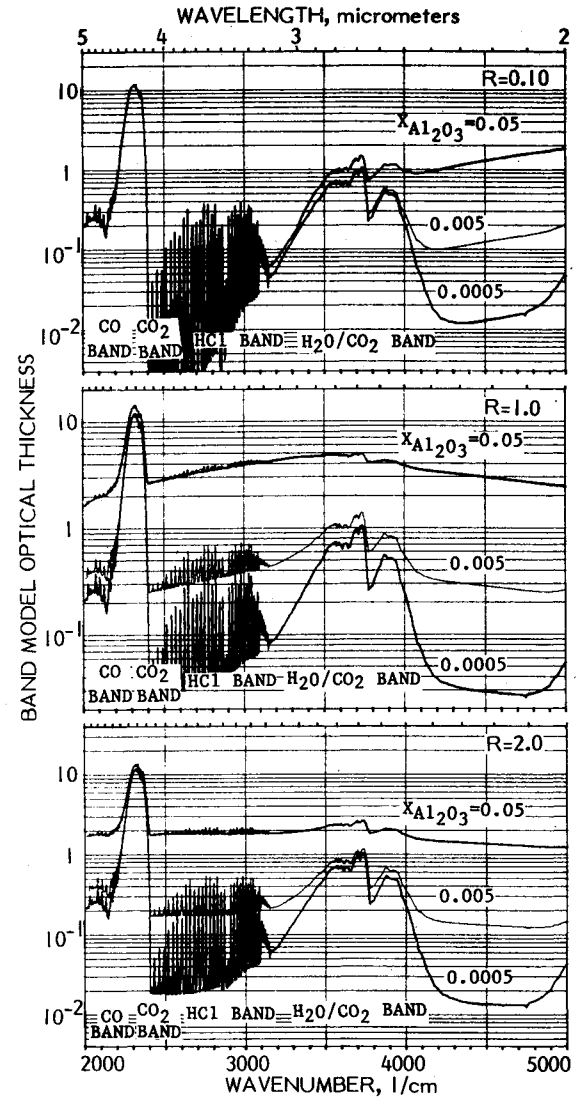

Fig. 9 Spectral variation of the band model optical thickness across the plume diameter for RSP at mole fractions of 0.0005, 0.005, 0.05 for 0.10-, 1.0-, and 2.0-μm aluminum oxide particles.

absorption and the radiance decreases. This occurs only at very large concentrations of Al_2O_3 particles, because their scattering cross section is small in the spectral range.

Figure 10 shows the integrated emission in the 2000-5000 1/cm wavenumber band as a function of particle size and concentration. The trends are the same as those discussed above for LTMFP.

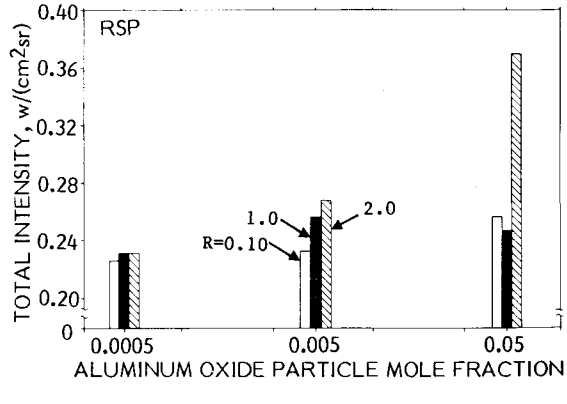

Fig. 10 Integrated radiative emission in the 2000-5000 1/cm wavenumber band from RSP as a function of particle size and concentration.

Advanced Minimum Smoke (ZrO_2/CO, H_2O, CO_2) Plume

The AMSP represents a typical plume from an advanced candidate minimum smoke propellant. The propellant contains zirconium carbide for combustion stability. The ZrC is converted to zirconium oxide particles in the combustion process. The mole fraction of ZrO_2 particles in the plume is usually less than about 5%. The minimum smoke propellant is a monopropellant in which the fuel and oxidizer exist together as a single chemical compound.

The spectral infrared radiance from the AMSP is shown in Fig. 11 for 0.1- and 1.0-μm particles at ZrO_2 mole fractions from 0.001 to 0.05. The plumes radiate like a blackbody in the 4.2-4.5-μm region due to the CO_2 gas emission.

The ZrO_2 particles have a very small absorption cross section in the infrared so that their albedo is essentially unity. Therefore, the infrared radiance is due mainly to the gases in the plume. Consequently, the local emission remains essentially constant for all particle loadings because the gas composition and temperature are constant.

Figure 12 shows the band model extinction optical thickness as a function of wavenumber for the plumes containing 0.1- and 1.0-μm ZrO_2 particles. The plumes containing 0.1-μm particles are optically thin except in the 4.3-μm CO_2 band.

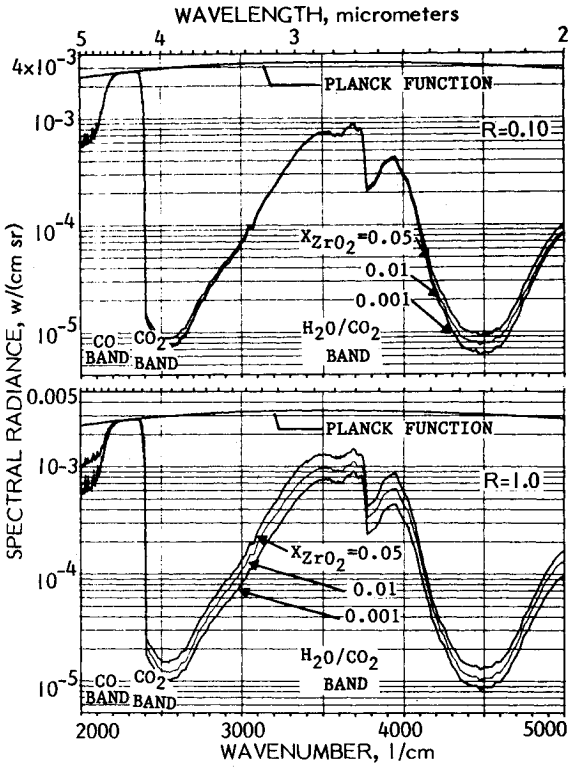

Fig. 11 Spectral radiance from AMSP at mole fractions of 0.001, 0.01, and 0.05 for 0.10- and 1.0-μm zirconium oxide particles.

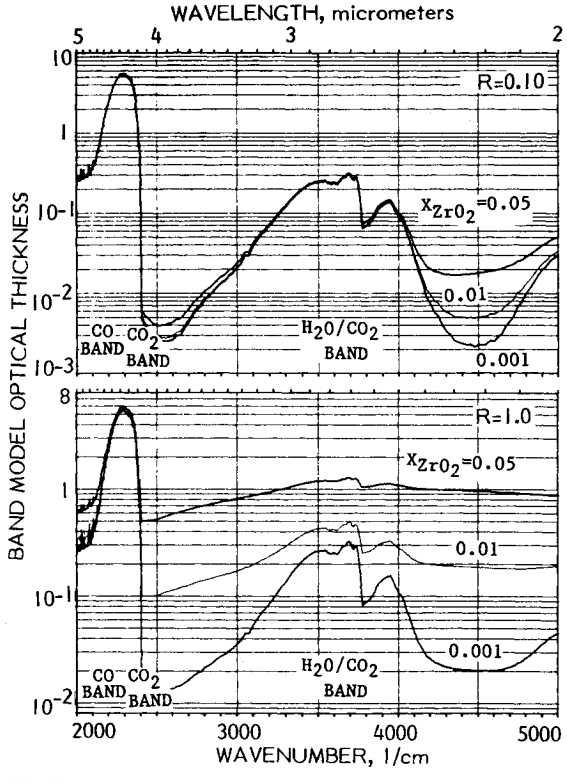

Fig. 12 Spectral variation of the band model optical thickness across the plume diameter for AMSP at mole fractions of 0.001, 0.01, and 0.05 for 0.10- and 1.0-μm zirconium oxide particles.

Also, the effect of the particles on η is very small except in the spectral regions near 2500 and 4500 1/cm, where the gas absorption is very small. Thus, the small particles have very little effect on the plume emission. The 1.0-μm particles influence the plume emission. This occurs because the addition of particles increases the plume emission when η is less than unity in the spectral regions where the plume albedo is less than unity. The plume radiates like a blackbody in the CO_2 4.3-μm band because absorption is very strong compared to scattering. In other words, the plume albedo is low in this spectral region.

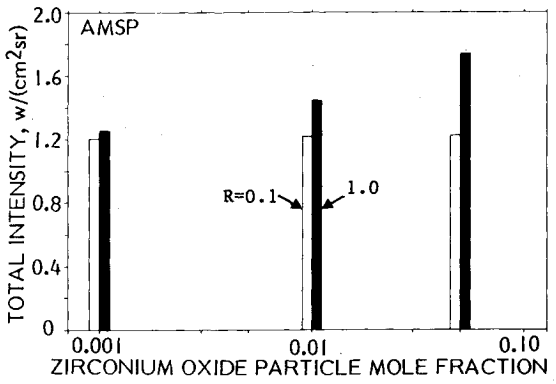

Fig. 13 Integrated radiative emission in the 2000-5000 1/cm wavenumber band from AMSP as a function of particle size and composition.

Figure 13 shows the total radiation emitted in the 2000-5000 1/cm wavenumber band as a function of ZrO_2 particle concentration and size. In general, the radiance from the AMSP is not very sensitive to the amount of ZrO_2 particulate for small particle sizes; however, it becomes increasingly sensitive to particle size and concentration as the particle loading increases.

Conclusions

A simplified model has been used to investigate the effects of scattering on the infrared radiation signature of four representative plumes. The simplified flowfield was used so that flowfield effects would produce a minimal influence on the radiation signatures when the particle size and concentration were changed.

The results for the advanced liquid rocket plume, which contains carbon particles, show that the spectral radiance and total intensity in the 2000-5000 1/cm wavenumber interval are both sensitive to the carbon particle mole fraction in the plume; however, they are insensitive to the particle size at a given carbon concentration. In other words the infrared signature is sensitive to the concentration of carbon in the plume and not to the size of the particles at a given carbon concentration. For the thermodynamic conditions considered in this study the carbon particle scattering masks the gaseous band spectrum for carbon particle mole fractions of 0.10 and greater.

The total intensity in the 2000-5000 1/cm wavenumber interval from the low-temperature metal fuel plume and the reduced smoke plume, both of which contain Al_2O_3 particles, is sensitive to the Al_2O_3 concentration. It generally increases with Al_2O_3 concentration until η reaches about unity and then decreases as the particle mole fraction is increased further. The total intensity is sensitive to particle size at a given Al_2O_3 concentration for particle mole fractions greater than 0.001. This occurs because the scattering cross section of the particles is very sensitive to particle size. The spectral radiance is insensitive to particle concentration at low particle mole fractions; however, as the particle mole fraction increases the signature at a given wavenumber may either increase or decrease, depending on the Al_2O_3 particle size and the plume optical thickness. In all the plumes with Al_2O_3 particles the maximum emission occurs in the gaseous bands. The 4.3-μm CO_2 band radiates like blackbody, so that the plumes emit a very strong signal near 4.3 μm.

The advanced minimum smoke plume contains low concentrations of ZrO_2 particles. The total intensity in the 2000-

5000 1/cm wavenumber band increases slightly with particle concentration and particle size at a given particle concentration. Also, because the particle mole fractions are low and the plume is optically thin, the spectral radiance increases slightly as the particle loading increases. The plume contains CO_2 which radiates like a blackbody at 4.3 μm.

The results of this investigation show that scattering influences the rocket plume infrared signatures. The magnitude of the influence depends on the type, concentration, and size of the particulate, as well as the wavelength of interest. The scattering calculations are dependent upon the particulate optical data. The SIRRM code contains the most current data available; however, in many cases the data is sparse and involves considerable extrapolation. There is a great need to increase the data base for the complex index of refraction of particulates that are of interest in plumes at realistic temperatures. In addition, the SIRRM data base needs to be extended to include coated particles.

References

[1]Goulard, R., ed., "Molecular Radiation and its Application to Diagnostic Techniques," NASA TM X-53711, Oct. 1967.

[2]Rochelle, W.C., "Review of Thermal Radiation from Liquid and Solid Propellant Rocket Exhausts," NASA TM X-53579, Feb. 1967.

[3]Edwards, D.K. and Bobco, R.P., "Effect of Particle Size Distribution on the Radiosity of Solid Propellant Rocket Motor Plumes," *Progress in Astronautics and Aeronautics: Spacecraft Radiative Transfer and Temperature Control*, Vol. 83, edited by T.E. Horton, AIAA, New York, 1982, pp. 111-127.

[4]Pearce, B.E., "Radiative Heat Transfer within a Solid-Propellant Rocket Motor," *Journal of Spacecraft and Rockets*, Vol. 15, March-April 1978, pp. 125-128.

[5]Lyons, R.B., Wormhoudt, J., and Kolb, C.E., "Calculation of Visible Radiation from Missile Plumes," *Progress in Astronautics and Aeronautics: Spacecraft Radiative Transfer and Temperature Control*, Vol. 83, edited by T.E. Horton, AIAA, New York, 1982, pp. 128-148.

[6]Lyons, R.B., Wormhoudt, J., and Gruninger, J., "Scattering of Radiation by Particles in Low Altitude Plumes," *Journal of Spacecraft and Rockets*, Vol. 20, March-April 1983, pp. 189-192.

[7]Young, S.J., "Retrieval of Flow Field Gas Temperature and Concentration in Low-Visibility Propellant Rocket Exhaust Plumes," AIAA Paper 81-1054, 1981.

[8]Staylor, W.F., "Determination of Stack Plume Properties from Satellite Imagery," *Journal of Spacecraft and Rockets*, Vol. 15, March-April 1978, pp. 92-99.

[9]Ludwig, C.B., Malkmus, W., Freeman, G.N., Reed, R., and Slack, M., "Infrared Radiation from Rocket Plumes," Technical Symposium, Society for Optical Engineering, SPIE, Vol. 253, *Modern Utilization of Infrared Technology VI*, 1980, pp. 122-128.

[10]Malkmus, W. and Reed, R., "Practical Treatment of Particle Plumes," Technical Symposium, Society for Optical Engineering, SPIE, Vol. 253, *Modern Utilization of Infrared Technology VI*, 1980, pp. 129-137.

[11]Ludwig, C.B., Malkmus, W., Walker, J., Slack, M., and Reed, R., "A Theoretical Model for Absorbing, Emitting and Scattering Plume Radiation," *Progress in Astronautics and Aeronautics: Spacecraft Radiative Transfer and Temperature Control*, Vol. 83, edited by T.E. Horton, AIAA, New York, 1982, pp. 111-127.

[12]Ludwig, C.B., Malkmus, W., Walker, J., Freeman, G.N., Reed, R., and Slack, M., "Standardized Infrared Radiation Model (SIRRM), Volume 1: Development and Validation," AFRPL-TR-81-54, 1981.

[13]Meador, W.E. and Weaver, W.R., "Six-Beam Models in Radiative Transfer Theory," *Applied Optics*, Vol. 15, Dec. 1976, pp. 3155-3160.

[14]Konopka, W., Reed, R.A., Calia, V.S., and Oman, R.A., "Controlled Hot Gas/Particle Experiments for Validation of a Standardized Infrared Model," AFRPL-TR-81-44, 1981.

[15]Nelson, H.F., "Scattering of Infrared Radiation in Rocket Exhaust Plumes," AFRPL-TR-82-015, 1982.